Journal of Chemical Health Risks
www.jchr.org
JCHR (2025) 15(6), 107-116 | ISSN:2251-6727

Synthesis, Spectral Studies, Corrosion Inhibition Potential, Density Functional Theory Calculations and Molecular Docking Simulation of CU(II) Complexes having Pentadentate Schiff Base Ligand

T. Varalakshmi, S. Praveen & Kannappan Geetha*

PG & Research Department of Chemistry, Muthurangam Government Arts College(Autonomous) Vellore - 632002, Affiliated by Thiruvalluvar University

(Received: 27 September 2025 Revised: 05 October 2025 Accepted: 01 November 2025)

KEYWORDS

Schiff base ligand – Corrosion inhibition DFT Calculations - HOMO–LUMO analysis – Molecular docking.

Abstract

A pentadentate Schiff base ligand and its binuclear copper(II) complexes were synthesized from 2,6-diformyl-4-methylphenol and 4-nitro-o-phenylenediamine in a 1:2 molar ratio. The ligand, with N_2O_3 donor sites, coordinates with two Cu(II) ions after phenolic deprotonation. Structural characterization by ^1H NMR, ^{13}C NMR, IR, UV–Vis, ESR, and conductivity measurements confirmed non-electrolytic behavior in DMF and supported a square planar geometry for the Cu(II) centers. Corrosion inhibition studies on mild steel in 0.1 N HNO_3 at 298 K showed high efficiency, attributed to adsorption of the compounds and formation of a protective barrier layer. Density functional theory calculations, including electrostatic potential mapping, HOMO–LUMO energy gap analysis, and Mulliken charges, were consistent with experimental observations. Molecular docking with the human estrogen receptor and breast cancer-associated protein (PDB ID: 5GIX) revealed favourable binding interactions, indicating potential biological activity of the Cu(II) complexes.

1. INTRODUCTION

Schiff bases are a class of compounds produced through the condensation of primary amines with carbonyl substrates, leading to the formation of the characteristic azomethine (–CH=N–) functional group. These molecules are widely recognized for their diverse biological activities, including antimicrobial, antiviral, antifungal, and antipyretic effects [2,3]. In coordination chemistry, Schiff bases are employed extensively as ligands, with the properties of their transition metal complexes strongly influenced by the structural features of the ligands themselves [4–7]. Their stability, ease of synthesis, and structural resemblance to natural biomolecules further enhance their utility in analytical applications and device fabrication [12,13]. The azomethine linkage has also been identified as a critical contributor to the biological efficacy of numerous natural and synthetic compounds [14–16]. In recent years, Schiff bases have also emerged as promising agents in corrosion inhibition for mild steel. Corrosion-resistant

Journal of Chemical Health Risks
www.jchr.org
JCHR (2025) 15(6), 107-116 | ISSN:2251-6727

coatings prepared from such compounds can effectively reduce the rate of steel degradation and enhance material longevity. Traditional organic inhibitors, though efficient, are often costly, which restricts their broader application [17]. The inhibition mechanism typically involves the transfer of electron density from the donor atoms or functional groups within the inhibitor molecule to the vacant d-orbitals of the metal surface, resulting in the formation of coordination complexes with geometries such as octahedral, tetrahedral, or square planar [18]. Once adsorbed onto the steel surface, these inhibitors create a protective film that prevents corrosive species from reaching active sites [19-22]. The adsorption process is largely determined by the physicochemical nature of the steel, the composition of the electrolyte, and the molecular characteristics of the inhibitor [23,24]. Furthermore, Schiff base molecules may directly interact with iron atoms on the mild steel surface to generate stable inorganic complexes, thereby reinforcing the protective barrier and further suppressing the corrosion process [25].

2. MATERIALS & METHODS

UV–Vis spectra of the ligand and complexes (1×10^{-3} M, 200–800 nm) were recorded on a Lambda-35 double-beam spectrophotometer. FTIR spectra were obtained with a Shimadzu instrument using KBr pellets (4000 – 400 cm^{-1}). Molar conductance measurements in DMF (1×10^{-3} M) were carried out with an Equiptronics EQ-665 conductivity meter. ^{1}H and ^{13}C NMR spectra of the ligands were recorded in DMSO-d_6 with TMS as reference on a Bruker Avance II 400 MHz spectrometer. Molecular weights were determined by HR-LC–MS (Waters Xevo G2-XS QToF). ESR spectra of the complexes were measured at room temperature on Bruker EMX X-band and Jeol ES-FA series spectrometers, with DPPH as standard (g = 2.003).

2.1 Computational details

The Gaussian09 software package has been extensively employed for quantum chemical investigations owing to its capability to provide reliable and accurate predictions of molecular properties [26]. In the present study, molecular geometry optimization and reactivity analyses were performed using the density functional theory (DFT) method with the B3LYP functional in conjunction with the 6-311++G(d,p) basis set [27]. Within this computational framework, several quantum chemical descriptors were evaluated, including frontier molecular orbital (HOMO–LUMO) energies, molecular electrostatic potential (MEP) mapping, Mulliken atomic charge distribution**,** and optimized structural parameters.

2.2 Molecular Docking

Molecular docking has emerged as a valuable computational strategy in drug discovery, offering the potential to accelerate pharmaceutical development while simultaneously reducing experimental time and cost. This method, which has gained prominence in recent years, enables the prediction of binding orientations between a ligand and its target protein [28]. In the present study, docking analyses were performed using the AutoDock 4.2.6 software package, with the resulting protein–ligand interactions and three-dimensional conformations visualized through PyMOL

Journal of Chemical Health Risks
www.jchr.org
JCHR (2025) 15(6), 107-116 | ISSN:2251-6727

[29]. A target protein with reported anticancer relevance was identified from the literature, and its crystal structure (PDB ID: 5GIX) was obtained from the Protein Data Bank**.** For docking preparation, the protein was refined using AutoDock Tools**,** during which co-crystallized ligands, water molecules, and cofactors were removed. Furthermore, Kollman charges and Gasteiger charges were applied, and polar hydrogens were incorporated to optimize the protein structure for subsequent docking studies [30].

2.3 Corrosion inhibition

The anticorrosive performance of copper(II) complexes was assessed using mild steel binding wire as the working material. The steel samples were purchased from a local supplier and subjected to surface treatment prior to testing. Initially, the wires were polished with emery paper, then washed successively with ethanol, acetone, and distilled water. After drying, they were placed in an oven at 120°C for one hour and weighed to record the initial mass. 20 ml of 0.1N HNO_3 were taken in the beaker No. 1, 20 ml of 0.1N HNO_3 and 25 mg of Schiff base ligand were added to beaker No. 2, 25 mg of the synthesised complexes (C**1** – C**5**) and 20 ml of 0.1N HNO_3 were added correspondingly, to the specified beakers numbered 3, 4, 5, 6, and 7. The pretreated specimens were subsequently immersed for 48 hours in a 0.1 N HNO_3 solution containing the synthesized complexes. Following exposure, the wires were withdrawn, repolished with emery sheets, rinsed thoroughly with distilled water, degreased with acetone, oven-dried, and weighed again to determine mass loss. All experiments were conducted in duplicate, and the average results were used for further analysis.

2.4 Preparation of Dinuclear Copper(II) Complexes

Dinuclear Copper(II) complexes were synthesized from the Schiff base ligand, NaOH, copper(II) salts, and $NaClO_4$ in a 1:1:1:2 molar ratio. The ligand (1 mmol, 0.43 g) was deprotonated with NaOH (1 mmol, 0.04 g) under stirring for 15 min, followed by the addition of copper(II) *p*-benzoate (1 mmol, 0.64 g) and further stirring for 45 min. $NaClO_4$ (2 mmol, 0.28 g) was then introduced, and the reaction mixture was stirred for 5 h. The resulting solid (Complex 1) was isolated by filtration, dried, and washed with ethanol. All other Complexes were obtained analogously using alternative Copper(II) precursors.

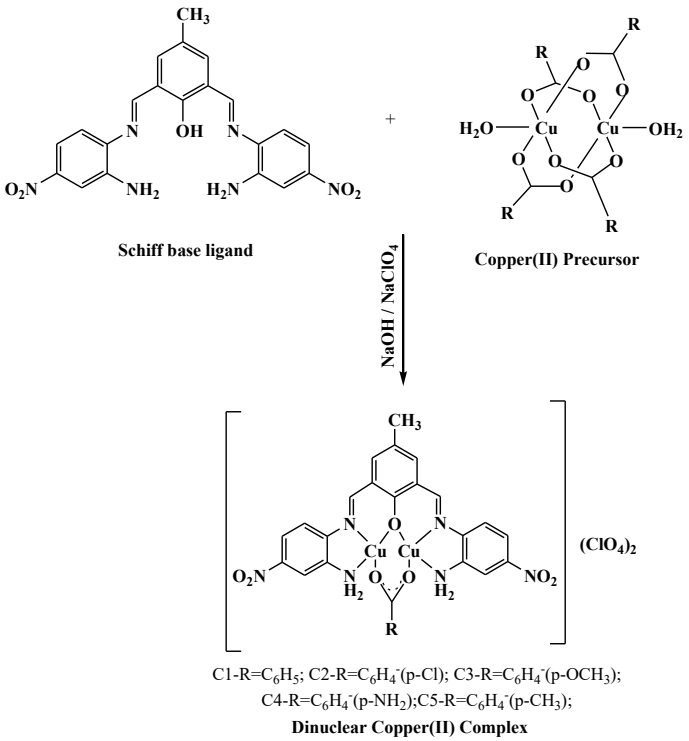

Schematic representation of preparation of dinuclear Copper(II) complexes

Journal of Chemical Health Risks
www.jchr.org
JCHR (2025) 15(6), 107-116 | ISSN:2251-6727

3. RESULT & DISSCUSSIONS

3.1 Uv-Visible Spectra

In the UV–Vis spectrum of the free ligands, an intense band around 270 nm can be assigned to the π–π* electronic transition of the aromatic phenyl moiety. A second band is observed at 356 nm, which is characteristic of the π–π* transition of the azomethine chromophore. In addition, a broader absorption feature at approximately 406 nm corresponds to the n–π* transition associated with the azomethine group. Upon coordination to metal ions, notable spectral modifications are observed. The second band is shifted to a slightly higher wavelength (362 - 366 nm), indicating perturbation of the azomethine π-system upon complexation. This shift is accompanied by an increase in absorption intensity, consistent with enhanced conjugation and stabilization of the excited state. The third band, now appearing in the 432 - 434 nm region, is still ascribed to n–π* transitions of the azomethine unit but shows a slight red-shift relative to the free ligand, further confirming the involvement of the azomethine nitrogen in coordination. Additionally, new absorptions emerge in the lower-energy region (455–484 nm), which are absent in the spectra of the uncoordinated ligands. These bands are attributed to ligand-to-metal charge transfer (LMCT) processes, reflecting electronic communication between the donor atoms of the ligand framework and the vacant orbitals of the central metal ion. The overall bathochromic shifts and the appearance of LMCT bands provide strong evidence for successful complex formation and support the coordination of the azomethine group to the metal centers.

3.2 Infrared Spectra

The azomethine (–HC=N) stretching vibration of the free Schiff base ligand is observed at 1622 cm^{-1}. Upon coordination with metal ions, this band undergoes a downward shift, reflecting the involvement of the azomethine nitrogen in complex formation through donation of electron density to the metal center. Consequently, the characteristic absorption of the C=N group in the complexes appears in the 1610 –1608 cm^{-1} region. A broad band around 3400 cm^{-1} is attributed to N–H stretching vibrations, which persist in all copper(II) complexes. The band at 1211 cm^{-1} is assigned to phenolic C–O stretching [31-33]. Additionally, a distinct absorption at 3053 cm^{-1} is associated with the hydroxyl group in the ligand; however, this band disappears after complexation, confirming deprotonation of the phenolic –OH and subsequent coordination of the oxygen donor site to the central metal ion.

3.3 ^{1}H NMR & ^{13}C NMR Spectra

The structural features of the synthesized Schiff base ligand were confirmed by detailed NMR analysis. In the ^{1}H NMR spectrum, a sharp singlet at δ 2.45 ppm was assigned to the methyl substituent on the aromatic ring, while the multiplet observed in the region δ 6.9 – 7.6 ppm corresponded to the aromatic protons. A distinct singlet at δ 8.8 ppm was attributed to the azomethine (-CH=N-) proton, providing direct evidence for the successful condensation reaction leading to Schiff base formation. The spectrum also displayed a broad signal at δ 13.7 ppm due to the phenolic –OH proton, as well as a resonance at δ 4.2 ppm that can be ascribed to amino ($-NH_2$) protons. The ^{13}C NMR spectrum further

Journal of Chemical Health Risks
www.jchr.org
JCHR (2025) 15(6), 107-116 | ISSN:2251-6727

corroborated the structural assignment. The signal at δ 164.8 ppm was characteristic of the azomethine carbon, while the carbon atom bonded to the hydroxyl group appeared at δ 159.4 ppm. The aromatic carbons resonated within δ 119.9–147.5 ppm, consistent with reported values for substituted aromatic systems. The methyl carbon was clearly identified at δ 20.98 ppm. Importantly, the resonance at δ 152.7 ppm indicated the presence of a nitro substituted carbon, thereby confirming the retention of nitro functionality within the ligand framework.

3.4 Mass Spectra

The mass spectrometric analysis provides strong evidence for the successful synthesis of the ligand and its metal complex. The Schiff base ligand exhibits a prominent molecular ion peak at m/z 435.62**,** which corresponds to its calculated molecular weight and is consistent with the molecular formula $C_{21}H_{18}N_6O_5$. In the case of the copper(II) complex (C1), the mass spectrum displays a parent ion peak at m/z 882.78**,** in excellent agreement with the theoretical molecular mass of the complex. The close correspondence between the experimental and calculated values confirms the identity and formation of both the free ligand and its copper(II) complex.

3.5 ESR Spectra

The measured g values of the copper(II) complexes were found to be higher than the free electron value (g = 2.0023). Such deviations are characteristic of Jahn–Teller distortions, which typically occur in Cu(II) systems due to their preference for an axially elongated geometry. The trend in the observed g values, namely $g\parallel > g\perp > 2.0023$ clearly indicates that the unpaired electron is localized in the $dx^2 - y^2$orbital [34]. Additionally, the condition $g\parallel > g\perp > 2.0023$ reflects a considerable degree of covalency in the metal–ligand bonding interactions, further supporting the electronic configuration and symmetry assignment of the complexes.

4. CORROSION INHIBITION

The adsorption of inhibitor molecules on the metallic surface results in the formation of a protective barrier that suppresses the active dissolution of the substrate. The rapid adsorption process ensures that the surface is effectively shielded from aggressive corrosive species. This interaction is facilitated through electron transfer from the inhibitor to the vacant low-energy orbitals of the metal, giving rise to coordinate bonding. Copper ions are particularly prone to coordination with donor ligands containing oxygen and nitrogen atoms. Consequently, Schiff base ligand bind to copper centers through phenolic oxygen and imine nitrogen functionalities, thereby promoting adsorption onto the metal surface.The inhibition performance is primarily influenced by the molecular size, electronic configuration, and structural features of the organic moiety.

5. DFT STUDIES

5.1 Molecular Electrostatic potential

The molecular electrostatic potential (MEP) map was obtained at the B3LYP/6-311+G(d,p) level to gain insights into the charge distribution and reactive sites of the molecule (Figure 2). The color code ranges from red (most negative) to blue (most positive), with green regions representing areas of near-zero potential. The highly negative regions (red)

Journal of Chemical Health Risks
www.jchr.org
JCHR (2025) 15(6), 107-116 | ISSN:2251-6727

are mainly localized around the oxygen atoms of the nitro and phenolic groups, which indicates that these positions are the most favorable for electrophilic attack.

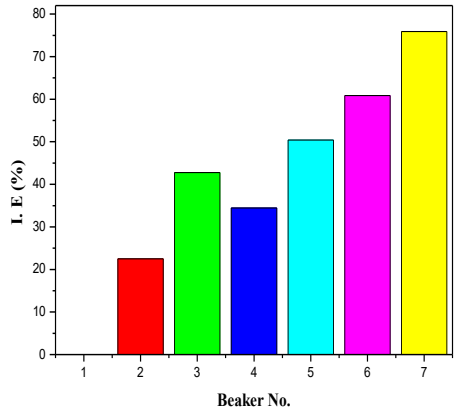

Figure 1: Inhibition Efficiency of Ligand and its Copper(II) Complexes.

The positive potential regions (blue) are concentrated over the hydrogen atoms of the aromatic and imine fragments, marking them as favorable sites for nucleophilic attack. The moderately negative and neutral regions (yellow to green) distributed across the aromatic rings reflect electron delocalization, which contributes to the molecule's conjugation and stability. This analysis highlights the role of nitro–oxygen and hydroxyl–oxygen atoms as strong electron-withdrawing centers, while the azomethine hydrogens act as potential donor sites. Such features are consistent with the general behavior of Schiff base derivatives and confirm the usefulness of MEP mapping in predicting reactive sites [35]

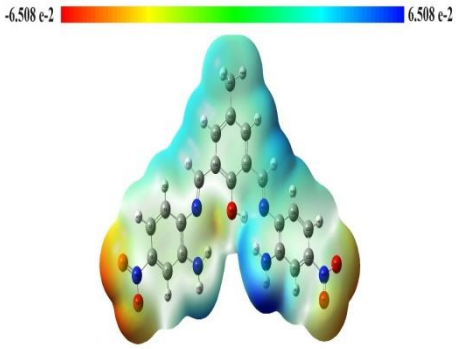

Figure 2: MEP map of Schiff base ligand

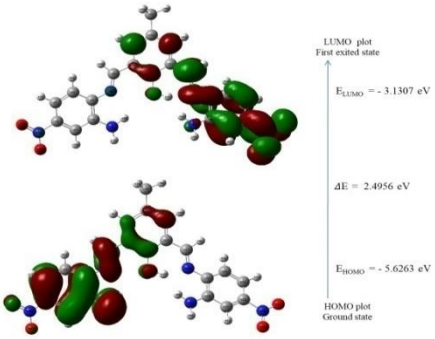

Figure3: Frontier molecular orbitals of Schiff base ligand

5.2 Frontier molecular orbitals

The frontier molecular orbital (FMO) analysis was carried out to evaluate the electronic properties and chemical reactivity of Schiff base ligand. The optimized HOMO and LUMO distributions are illustrated in Figure 3, while the corresponding energy parameters are summarized in Table 1. The calculated HOMO energy is –5.6263 eV and the LUMO energy is –3.1307 eV, giving an energy gap (ΔE) of 2.4956 eV. This relatively small gap suggests moderate chemical reactivity and good electronic communication across the conjugated system, which is favorable for charge transfer processes. The ionization potential (5.6263 eV) and electron affinity (3.1307 eV) were derived directly from the HOMO and LUMO values, respectively.

Journal of Chemical Health Risks
www.jchr.org
JCHR (2025) 15(6), 107-116 | ISSN:2251-6727

Additional global reactivity descriptors such as electronegativity (4.3785 eV), chemical potential (–4.3785 eV), chemical hardness (1.2478 eV), chemical softness (0.4007 eV), and electrophilicity index (7.6820 eV) further indicate that the molecule possesses a significant ability to accept electrons, consistent with its π-conjugated framework [36]. These findings confirm that the electronic configuration of Schiff base ligand facilitates efficient intramolecular charge transfer, supporting its potential application in optoelectronic and biological systems.

5.3 Mulliken atomic charges

The electronic structure and reactivity of Schiff base ligand were examined through Mulliken atomic charge analysis, performed at the DFT/B3LYP/6-311++G(d,p) level of theory.

Table 1: The calculated Frontier molecular orbitals of Schiff base ligand

Parameters	Values
HOMO(eV)	-5.6263
LUMO(eV)	-3.1307
Ionization potential	5.6263
Electron affinity	3.1307
Energy gap(eV)	2.4956
Electronegativity	4.3785
Chemical potential	-4.3785
Chemical hardness	1.2478
Chemical softness	0.4007
Electrophilicity index	7.6820

The results indicate that nitrogen atoms (N1, N8, N18, N28) carry significant negative charges (-0.40 to -0.68 e), highlighting them as nucleophilic centers, whereas oxygen atoms (O26, O27, O29, O48, O49) also possess substantial negative charges (-0.26 to -0.56 e), suggesting their involvement in hydrogen bonding and potential coordination interactions. Carbon atoms display a mixed distribution of positive and negative charges, reflecting bond polarization and electronic delocalization within the molecular framework, while hydrogen atoms are positively charged (0.125–0.384 e), consistent with their role as proton donors in intramolecular interactions. The charge distribution pattern provides insight into the reactivity, stability, and possible sites for electrophilic or nucleophilic attack, which can influence molecular docking and biological activity. These findings are consistent with previous studies on similar Schiff base derivatives, where charge localization and electronic polarization were found to govern molecular interactions and reactivity [37].

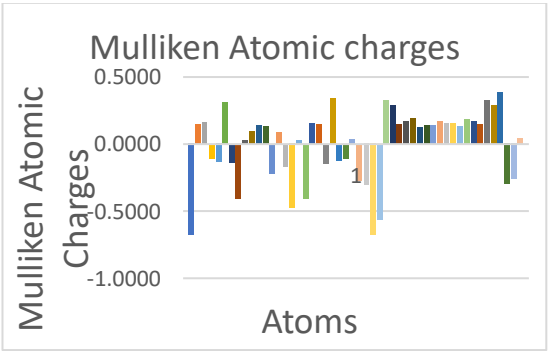

Figure 3: The histogram of Mulliken atomic charges of Schiff base ligand

6. MOLECULAR DOCKING

The binding orientation of C1-C5 complexes provides a summary of the docking results.

Journal of Chemical Health Risks
www.jchr.org
JCHR (2025) 15(6), 107-116 | ISSN:2251-6727

With favourable binding energies ranging from -7.60 to -8.21 kcal/mol, all complexes demonstrated a strong affinity for the 5GIX active site residues. With a binding energy of -8.21 kcal/mol, an intermolecular energy of -9.11 kcal/mol, and the lowest inhibition constant (955 nM), Complex C5 had the best docking profile of all the examined complexes. These numbers imply that Complex C5 has the highest inhibitory potential and the strongest connection. The amino acid residues LYS12, LEU14, LYS159, ASN18, ASP562, and LYS560 were important in the binding process. Numerous hydrogen bonding interactions (H–O, O–H) and metal coordination bonds (Cu–O) between the ligand and the protein residues were discovered by the docking study. Cu–O coordination is very crucial because it keeps the ligand in the binding pocket and may increase biological activity.

7. CONCLUSION

The structural features of the synthesized Schiff base ligands and their Cu(II) complexes were confirmed by a combination of spectroscopic and computational methods. UV–Vis, FT-IR and NMR spectra verified the formation of the Schiff bases, while ESR data supported square-planar geometries with unpaired electrons localized in the d(x^2–y^2) orbital. Mass spectrometry and conductivity results further validated the proposed structures. DFT calculations at the B3LYP/6-31G(d,p) level provided optimized geometries, Mulliken charges, and HOMO–LUMO gaps, in agreement with experimental findings. These results collectively demonstrate the pentadentate coordination mode of the ligands and the electronic stability of the Cu(II) complexes. Among the tested compounds, copper(II) complexes bearing methyl (-CH_3) substituent exhibit the highest inhibition efficiency. This enhanced protective ability can be ascribed to the abundance of electron-rich centres, including oxygen, nitrogen, and delocalized π-electrons, which effectively block the active sites of mild steel and restrict its interaction with the corrosive medium. The RMSD values for the docking poses were found to be consistent (~ 41– 42 Å) for most complexes, suggesting reliable conformational stability, with the exception of Complex C3 which showed a higher RMSD (102.88 Å), indicating structural deviation and lower stability. Overall, the docking study demonstrates that Complex C5 forms the most stable and energetically favorable complex with 5GIX, supported by strong hydrogen bonding, Cu–O interactions, and low inhibition constant. Complexes C1 and C2 also showed comparable affinity with Ki values near 1 μM, while Complexes C3 and C4 exhibited relatively weaker interactions. These findings highlight the potential of the optimized ligand, particularly in Complex C5, as a promising candidate for further biological evaluation.

REFERENCES

1 Ahamad I, Prasad R, Quraishi MA, Corrosion Sciences 52:933–942, (2010).

2 Amin MA, Khaled KF, Mohsen Q, Arida HA, Corrosion Sciences 52:1684–1695, (2010)

3 Anitha C, Sheela CD, Tharmaraj P, Shanmugakala R, International Journal Inorganic Chemistry 2013:1–10, (2013)

Journal of Chemical Health Risks

www.jchr.org

JCHR (2025) 15(6), 107-116 | ISSN:2251-6727

4 Yıldırım A, Çetin M, Corrosion Sciences 50:155–165, (2008)

5 Emregul KC, Hayvalı M Mater Chem Phys 83:209–216, (2004)

6 Solmaz R, Electrochim Acta 53:5941–5952, (2008)

7 Bockris JO, Swinkels DAJ, Journal of Electrochemical Society 111:743–748, (1964)

8 Branzoi V, Branzoi F, Baibarac M, Mater Chem Phys 65:288–297, (2000)

9 Oguzie EE, Li Y, Wang FH, Journal Colloid Interface Sci 310:90–98, (2007)

10 Alijourani J, Raeissi K, Golozar MA, Corrosion Sciences, 51:1836–1843, (2009)

11 Obot IB, Obi-Egbedi NO Corrosion Sciences, 52:198–204, (2010).

12 Li, Corrosion Sciences, 48:308–321, (2006)

13 Kadhum A, Mohamad AB, Hammed L, Al-Amiery AA, San NH, Materials 7:4335–4348, (2014)

14 D.N. Dhar and C.L. Taploo, J. Sci. Ind. Res. 41, 501–506, (1982)

15] P. Przybylski, A. Huczyński, K. Pyta, B. Brzezinski and F. Bartl, Curr. Org. Chem. 13, 124–148 (2009).

16 P.J. Bhattacharya, Indian Chem. Soc. 59, 505 (1982).

17 C.R. Samy, Indian J. Chem. 35 (A), 1 (1996).

18 X. Shen, Q.I.C. Yang and Y. Xie, Synth. React. Inorg.Met.Org. Chem. 26, 1135–1147 (1996).

19 K. Singh, S.N.Dubey and J.P. Tandon, Synth. React. Inorg.Met. Org. Chem. 23, 1251–1258 (1993).

20 A.A. Nejo, G.A. Kolawole and A.O. Nejo, J. Coord. Chem.63 (24), 4398–4410 (2010).

21 R. Vafazadeh and M. Kashfi, Bull. Korean Chem. Soc. 28(7), 1227–1230 (2007).

22 N. Raman, J.D. Raja and A. Sakthivel, J. Chem. Sci. 119(4), 303–310 (2007).

23 L.C. Nathan, J.E. Koehne, J.M. Gilmore, K.A. Hannibal,W.E. Dewhirst and T.D.Mai, Polyhedron. 22 (6), 887–894(2003).

24 S. Patai, The Chemistry of the Carbon-Nitrogen Double Bond (J.Wiley and Sons, New York, 1970).

25 E. Jungreis and S. Thabet, Analytical Applications of Schiff bases (Marcell Dekker, New York, 1969).

26 G. Bringmann, M. Dreyer, J.H. Faber, P.W. Dalsgaard, D.Staerk and J.W. Jaroszewski, J. Nat. Prod. 67 (5), 743–748 (2004).

27 J. Salimon, N. Salih, H. Ibraheem and E. Yousif, Asian J.Chem. 22 (7), 5289–5296 (2010).

28 Z. Guo, R. Xing, S. Liu, Z. Zhong, X. Ji, L. Wang and P. Li, Carbohydr. Res. 342 (10), 1329–1332 (2007).

29 J. A. Pople and Sir John Lennard-Jones, Proc. Roy. Soc.A 202, 166-180, (1950).

Journal of Chemical Health Risks

www.jchr.org

JCHR (2025) 15(6), 107-116 | ISSN:2251-6727

30 N.M. O'Boyle, AL Tenderholt, KM Langer, J. Comput. Chem. 29, 839-845, (2008),

31 S. Praveen, K. Geetha et al., Applied Organometallic Chemistry,; 39:e7984, (2025).

32 R. Prabakarakrishnan, S. Praveen, K. Geetha et al.,Environmental Research 201, 111520, (2021).

33 S. Praveen & K. Geetha et al., Scientific Reports, 15: 6957, (2025).

34 A. Nagajothi, A. Kiruthika, S. Chitra and K. Parameswari, Res. J.Chem. Sci., 3, 35, , (2013).

35 Scrocco, E., & Tomasi, J., Advances in Quantum Chemistry (Vol. 11, pp. 115–129). Academic Press, (1978).

36 Chattaraj, P. K., Roy, D. R., & Subramanian, V., The Journal of Physical Chemistry A, 110(20), 6531–6536, (2006).

37 **Khalaji, M., Khosravi, M., &Ghaedi, M.,** *Journal of Molecular Structure, 1210*, 128004, (2020).